CORA Cork Open Research Archive
Cartlann Taighde Oscailte Chorcaí

Title	Isotropic and anisotropic collision-induced Raman scattering by monoatomic gas mixtures: Ne-Ar
Author(s)	Dixneuf, Sophie; Chrysos, M.; Rachet, F.
Publication date	2009
Original citation	Dixneuf, S., Chrysos, M. and Rachet, F. (2009) 'Isotropic and anisotropic collision-induced Raman scattering by monoatomic gas mixtures: Ne-Ar', Physical Review A, 80(2), 022703. (8pp). doi: 10.1103/PhysRevA.80.022703
Type of publication	Article (peer-reviewed)
Link to publisher's version	https://journals.aps.org/pra/abstract/10.1103/PhysRevA.80.022703 http://dx.doi.org/10.1103/PhysRevA.80.022703 Access to the full text of the published version may require a subscription.
Rights	**© 2009, American Physical Society**
Item downloaded from	http://hdl.handle.net/10468/4533

UCC

University College Cork, Ireland
Coláiste na hOllscoile Corcaigh

Isotropic and anisotropic collision-induced Raman scattering by monoatomic gas mixtures: Ne-Ar

S. Dixneuf,[1,2] M. Chrysos,[1,*] and F. Rachet[1]

[1]*Laboratoire des Propriétés Optiques des Matériaux et Applications,*
UMR CNRS 6136, Université d'Angers, 2 Boulevard Lavoisier, 49045 Angers, France
[2]*Department of Physics, University College Cork, Cork, Ireland*
(Received 19 May 2009; published 7 August 2009)

We report the long-overdue collision-induced Raman scattering spectrum by a pair of unlike rare gas atoms. Absolute-unit scattering intensities, both isotropic and anisotropic, are given for Ne-Ar, along with the depolarization ratio for this system, recorded by a gaseous room-temperature mixture over a wide range of frequency shift. We make a critical comparison with spectra computed quantum-mechanically on the basis of modern pair-polarizability representations for Ne-Ar, of either *ab initio* or density functional theory methods. We report a value for the Kerr second virial coefficient, deduced from our measurements. Our data are especially intended to add to the vital yet hitherto incomplete knowledge of the role of collision-induced processes in atmospheric environments.

I. INTRODUCTION

In dense mixtures of atomic gases, two unlike colliding atoms can be viewed and studied as a free-heteronuclear pair, which unlike homonuclear pairs has a transient interaction dipole moment. The latter has been known and studied for over fifty years as responsible for the collision-induced absorption (CIA) bands observed by gas mixtures in the far infrared region of the electromagnetic spectrum [1–3]. So far, however, only little is known about the complementary process of collision-induced scattering (CIS) by atomic gas mixtures. The same is true also with the transient interaction polarizability responsible for that process, which until recently had been almost unknown in the quantum chemistry literature.

On another level, since the first measurements by McTague and Birnbaum in the late 60's [4,5], pure atomic gases inactive in CIA have been intensively and almost exhaustively investigated through CIS [6–8]. The related homonuclear-pair polarizabilities have been repeatedly measured or quantum-chemically calculated as a function of the interatomic distance, r.

Thanks in particular to the experimental know how of our group and to the Raman setup we have developed and constantly been improving over the last years to achieve higher and higher sensitivity, our group has measured extremely weak CIS signals. Such weak signals appear, for instance, in the very far wings of CIS gas spectra, such as the ones by monoatomic gases [9–16]. Exploring the most energetic transitions enables in turn to probe the closest separations of the interaction, where orbitals mix heavily and quantum-mechanical effects of orbital overlap and electron exchange have a great contribution.

On theoretical grounds, CIS intensities need accurate potential energy surfaces (PES) and pair-polarizability representations, both of which are functions of r [17,18]. In order to account properly for polarization, dispersion, induction, electron exchange and correlation effects and for orbital overlap, PES and electric properties for interacting closed-shell systems require expensive quantum-chemistry computations. Rare gas atomic pairs, in particular, form van der Waals (vdW) complexes that are kept stable exclusively by dispersion, which is solely a dynamic electron correlation effect [19]. The latter can only be properly accounted for at a full post-Hartree-Fock level, that is, with expensive numerical methods such as configuration interaction, perturbation theory, or coupled-cluster response approach. To be effective, these computations must be combined at least with "triple zeta valence" polarization basis sets augmented by diffuse orbitals. For the past ten years, the Dunning and coworkers' well-balanced correlation-consistent basis sets [20,21], which fulfill these requirements, have been successfully used to describe the interaction polarizability of vdW rare gas pairs as a function of separation [22–25].

Here, we report an exhaustive joint experimental and theoretical study of a mixture of two atomic gases (Ne : Ar) via CIS. The impulse for this work was some recently appearing *ab initio* computations for the pair polarizability of Ne-Ar [25,26], which present themselves as an opportunity to challenge our experimental and theoretical expertise to such a delicate class of systems. On experimental grounds, the difficulty of the task mainly relies upon the extraction of the Ne-Ar interactions from a weak binary signal, which unlike CIA contains contributions due also to the pairs of like atoms, $(Ne)_2$ and $(Ar)_2$, that are simultaneously probed.

Anisotropic and isotropic spectra for Ne-Ar are reported along with the depolarization ratio over a broad range of frequency shift. Experimental spectra and moments are straightforwardly compared with quantum-mechanical ones from various pair polarizability models (including the state-of-the-art coupled-cluster ones), most of which have never been checked before the present study. Main similarities and discrepancies between, on one hand, the heteronuclear pair polarizability models and the scattering intensity spectra and, on the other hand, their counterparts for the related homonuclear pairs are also briefly discussed.

─────────
*michel.chrysos@univ-angers.fr

As has been already pointed out by Rizzo and coworkers [27], neither Kerr nor refractivity or dielectric second virial coefficients had been measured for Ne-Ar at any temperature or exciting wavelength until 2006, and to the best of our knowledge this is now still the case three years later. For pairs of unlike atoms, some specific components of these macroscopic electrooptical parameters are related exclusively to the pair-polarizability tensor anisotropy or trace, and are therefore in close relation with the corresponding anisotropic or isotropic CIS intensities. Here, we report an experimental value for $B_K^{(0),\alpha^2}$ at 294.5 K [28], which is, at this temperature, by far the dominant contribution to the Kerr second virial coefficient, B_K, of Ne-Ar.

II. THEORETICAL

A. Intensities

For a pair of rare gas atoms the reliable calculation of CIS frequency-resolved spectra requires the most rigorous theoretical framework, that is, quantum mechanics. To convert coordinate-dependent polarizability to frequency-dependent CIS intensity, one has to superpose, over all possible values of the rotational quantum number, properly weighted energy-integrated squared matrix elements, according to formulas detailed in references [17,18]. The CIS intensity, anisotropic $I_\parallel$ or isotropic I_{iso}, is then expressed as:

$$I_\parallel(\nu) = \frac{2}{15} \frac{h^3 V}{Z_T} k_0 k_s^3 \langle g_J |\langle \psi_{J',E'} |\beta| \psi_{J,E}\rangle|^2 \rangle, \qquad (1)$$

$$I_{iso}(\nu) = \frac{h^3 V}{Z_T} k_0 k_s^3 \langle g_J |\langle \psi_{J',E'} |\alpha| \psi_{J,E}\rangle|^2 \rangle, \qquad (2)$$

where ν denotes frequency shift, Z_T is the partition function at temperature T, k_0 and k_s are the wavevector moduli for the incident and scattered electromagnetic fields, respectively, and $h^3 V$ is the phase-space normalization volume (with V the physical volume of the sample and h the Planck's constant); $\psi_{J,E}$ and $\psi_{J',E'}$ are the energy-normalized vibrational wavefunctions of the initial (E,J) and final (E',J') states of the pair, respectively, where E and E' denote energy and J and J' denote rotational quantum numbers. Functions $\alpha(r)$ and $\beta(r)$ stand for the incremental trace and anisotropy, which are the two invariants of the second-rank polarizability tensor of the pair. External brackets $\langle \cdots \rangle$ denote statistical averaging over energy and angular momentum for the quasi-molecule. Quantity g_J stands for nuclear statistical weight, taking values that depend on the parity of the rotational quantum number J.

For unlike pairs, the values of the parameters g_J and Z_T are no more the same as in the well-known case of a like pair. Even though this specific problem is part of a vast, well-documented area [29–31], some aspects on how to determine these values are novel and deserve some short explanation. In fact, while in the case of two like bosons the degeneracy of the either symmetric or antisymmetric nuclear spin function of the pair is $G_S = \Sigma_{\mathcal{T}=0,2,4,...}^{2\mathcal{I}} (2\mathcal{T}+1) = (\mathcal{I}+1)(2\mathcal{I}+1)$ and $G_A = \Sigma_{\mathcal{T}=1,3,5,...}^{2\mathcal{I}-1} (2\mathcal{T}+1) = \mathcal{I}(2\mathcal{I}+1)$, re-

spectively (with $\mathcal{I}$ the nuclear spin of the atom and $\mathcal{T}$ the nuclear spin of the pair), in the case of two unlike bosons the total wavefunction of the pair has no specific symmetry. As a result, unlike pairs of rare gas atoms ($\mathcal{I}=\mathcal{T}=0$) will assign to g_J the constant value $g_J = G_S + G_A = 1$, whereas like pairs assign to g_J the two distinct values $g_{0,2,4,...} = G_S = 1$ and $g_{1,3,5,...} = G_A = 0$ depending on whether J takes even or odd values.

For related reasons, Z_T will again depend on whether like or unlike pairs are considered. In fact, by approximating Z_T by the sum over the free states of the pair (with a total energy, the kinetic energy E_{kin}), one gets: $Z_T \approx g_J \int_{\mathcal{T}} e^{-E_{kin}/k_B T} d\tau$. After some elementary calculus, the latter integral reads: $V \int_{-\infty}^{\infty} \int_{-\infty}^{\infty} \int_{-\infty}^{\infty} e^{-\mathbf{p}^2/(2\mu k_B T)} d\mathbf{p} = V h^3 L^{-3}$, with $d\tau$ the phase-space volume element, $\mathbf{p}$ the linear momentum of the pair, μ the reduced mass, k_B the Boltzmann's constant, and $L = h/\sqrt{2\pi\mu k_B T}$ the thermal de Broglie wavelength. As a consequence, unlike pairs of rare gas atoms have a partition function taking the value $Z_T \approx g_{0,2,4,...} \frac{1}{2} V h^3 L^{-3} + g_{1,3,5,...} \frac{1}{2} V h^3 L^{-3} = V h^3 L^{-3}$, which is twice as great as the one for like pairs: $Z_T \approx g_{0,2,4,...} \frac{1}{2} V h^3 L^{-3} = \frac{1}{2} V h^3 L^{-3}$.

For this work, the vibrational wavefunctions, $\psi_{J,E}$, were built on a grid through a step-by-step propagation according to the Numerov's algorithm, subjected to appropriate boundary conditions [17]. For the Ne-Ar, Ne-Ne, and Ar-Ar interaction potentials $V(r)$, use was made of accurate, commonly recognized semiempirical Hartree-Fock plus dispersion models long-past established by the group of Aziz; that is, the respective two HFD-B models for the first two enumerated pairs [32,33] and the HFDTCS2 model for the third pair [34].

B. Pair-polarizability

The Ne-Ar pair-polarizability tensor trace α and anisotropy β have been computed by two different groups for several values of separation r.

(1) The group of Maroulis has reported two *ab initio* models, obtained either from coupled-cluster calculations, using single and double virtual electronic excitations with perturbative inclusion of triple excitations [CCSD(T)] (coupled-cluster with single, double, and connected triple excitations), or from a self-consistent-field (SCF) approximation. That same group has also reported a B3LYP (Beck-Lee-Yang-Parr exchange-correlation functional) model that is based on a density functional theory (DFT) calculation [26].

(2) More recently, Cacheiro and coworkers suggested another *ab initio* model, which is obtained from coupled-cluster calculations, using single and double virtual excitations (CCSD) [25].

Specifically, the group of Maroulis has implemented the methods SCF and B3LYP for two different couples of diffuse orbital basis sets [Ne/Ar] of near-Hartree-Fock quality, named A=[7s5p4d1f/8s6p5d3f] and B=[7s5p5d3f/8s6p5d4f] [26,35]. The CCSD(T) method has only been used in conjunction with the reduced basis set A. In what follows, the notations SCF, B3LYP, and CCSD(T) will refer to SCF/B, B3LYP/B, and CCSD(T)/A, respectively. Hättig and Cacheiro, and their colleagues have used a

d-aug-cc-pVQZ-33211 orbital basis set for both Ne and Ar atoms [22,23,25]. This acronym stands for a Dunning's correlation-consistent, polarized valence orbital basis set (cc-pV) that has been supplemented with four sets of polarization functions (QZ for quadrupole zeta) and augmented by two sets of diffuse functions (d-aug for doubly-augmented). These authors have also proposed to treat the pair-polarizability frequency dependence by expanding Cauchy moments to the second-order approximation in the frequency arguments [22,24]. The frequency-corrected model thus obtained at the laser frequency of our experiment will hereafter be referred to as $CCSD_\omega$.

The long-range classical dipole-induced dipole (DID) mechanism [36] was considered in order to extrapolate asymptotically the computed pair-polarizability functions. For a rare gas heteronuclear pair *ab*, the DID expressions for the pair-polarizability tensor anisotropy, β_{DID}, and trace, α_{DID}, read as follows:

$$\beta_{DID} = \frac{6\alpha_a\alpha_b}{r^3} + \frac{3\alpha_a\alpha_b(\alpha_a + \alpha_b)}{r^6} + \dots, \qquad (3)$$

$$\alpha_{DID} = \frac{2\alpha_a\alpha_b(\alpha_a + \alpha_b)}{r^6} + \dots, \qquad (4)$$

where a series expansion of β and α to the order r^{-6} was assumed, with α_a and α_b the static atomic polarizabilities of *a* and *b*. For the Maroulis' SCF, B3LYP, and CCSD(T) functions, the input atomic polarizabilities were obtained from consistent quantum-chemistry calculations, and were given the respective values: $2.3723a_0^3$, $2.8734a_0^3$, and $2.7149a_0^3$, for α_{Ne}; $10.6556a_0^3$, $11.5186a_0^3$, and $11.475a_0^3$, for α_{Ar} [26]. *B*-splines were used to guarantee the smoothness of the models during computation of intensities. For the Cacheiro's CCSD and $CCSD_\omega$ functions, no DID extension was necessary. Instead, use was made of their analytic functions P_{fit} [25], which fit reliably their models over the entire range [4.5:300] bohr.

Figure 1 illustrates Ne-Ar anisotropy [Fig. 1(a)] and trace [Fig. 1(b)] representations as a function of *r*. For comparison, the best models for the related homonuclear pairs are also shown, i.e., the CCSD functions by Hättig *et al.* for $(Ne)_2$ [23] and $(Ar)_2$ [22]. The latter have been calculated with the same orbital basis set as in the case of Ne-Ar [25]. The closest separation effectively probed by CIS spectroscopy at 294.5 K is at about 4, 4.5, and 5 bohr, for $(Ne)_2$, Ne-Ar, and $(Ar)_2$, respectively [37–39].

When comparing with one another the various Ne-Ar polarizability models, focusing in particular on the regions enhanced in the insets, one observes that SCF, which totally disregards dynamic electron correlation, goes underneath the other models and especially CCSD. This comparison is quite a useful tool, reflecting the extent to which dynamic electron correlation has been included at different levels of optimization. Although triple excitations accounted for through perturbation theory [CCSD(T)] indeed make β to be further increased with respect to CCSD, their impact on α is no longer positive. This may be attributed to the use by Maroulis of the reduced diffuse orbital basis A, not fully optimized
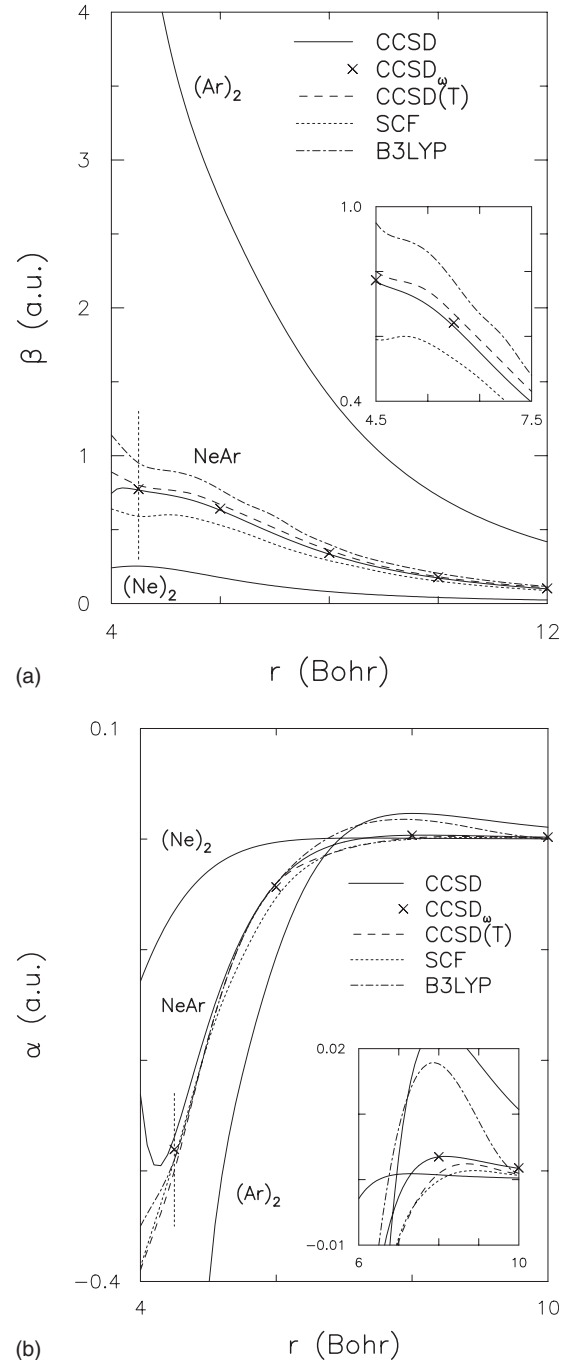

FIG. 1. Pair-polarizability functions of Ne-Ar (a_0^3) as a function of the interatomic distance (bohr): CCSD [25], $CCSD_\omega$ [25], CCSD(T) [26], SCF [26], and B3LYP [26]. The CCSD functions of $(Ne)_2$ [23] and $(Ar)_2$ [22] are also shown, for the sake of comparison. (a) anisotropy $\beta(r)$; (b) incremental trace $\alpha(r)$. Vertical dotted lines are used to show the minimum Ne-Ar separation effectively probed by CIS spectroscopy at room temperature.

for argon in particular [26]. Interestingly, frequency corrections ($CCSD_\omega$) provide only minor changes to static models (CCSD). Finally, DFT provides curves that go far above the ones obtained *ab initio*, even though they are all of the same shape.

III. EXPERIMENTAL

The CIS intensities were measured as a function of frequency shift ν by means of the right-angle Raman scattering setup described in Refs. [11,12]. In this experiment, one has the possibility of choosing whether the polarization of the incident laser beam is parallel ($\parallel$) or perpendicular ($\perp$) to the scattering plane. These options enable one to record two independent yet complementary signal components, so-called depolarized, $I_{\parallel}$ (also called anisotropic), and polarized, $I_{\perp}$. The particularly weak isotropic spectrum is then obtained from these two components through the combination [40,41]:

$$I_{iso} = I_{\perp} - \frac{7}{6}I_{\parallel} \qquad (5)$$

On experimental grounds, the depolarization ratio, $\eta(\nu)$, is defined as the ratio between the recorded quantities $I_{\parallel}$ and $I_{\perp}$. On theoretical grounds, it is rather obtained from the quantum-mechanically computed intensities, $I_{\parallel}$ and I_{iso}:

$$\eta = \frac{I_{\parallel}}{I_{iso} + \frac{7}{6}I_{\parallel}}. \qquad (6)$$

We define the gas mixture by the ratio $\gamma = \rho_{Ne}/\rho_{Ar}$, where ρ_{Ne} and ρ_{Ar} are the partial densities of the two gases (in amagat). For each value of ν, the recorded noise-corrected binary scattering signal, $S_{(2)}$, reads:

$$S_{(2)} = \frac{\rho_{Ne}^2}{2!}I_{NeNe} + \rho_{Ne}\rho_{Ar}I_{NeAr} + \frac{\rho_{Ar}^2}{2!}I_{ArAr}, \qquad (7)$$

where I_{NeNe}, I_{ArAr}, and I_{NeAr} are the density-independent intensities probing the interactions between two Ne atoms, between two Ar atoms, and between one Ne atom and one Ar atom, respectively. They, respectively, are weighted by $\rho_{Ne}^2/2!$, $\rho_{Ar}^2/2!$, and $\rho_{Ne}\rho_{Ar}$, that is, by the number densities of the two homonuclear atomic pairs in the mixture, and by the number density of the heteronuclear pairs.

All due care was taken to minimize parasitic scattering by monomers, i.e., impurities, atmospheric traces, as well as residual gaseous hydrogen used for calibration. To this purpose, industrial atomic gases with total residual impurities $<$10 ppm were used (company Air Liquide). For a mixture of a given γ, care was taken to guarantee that the contribution of any ternary collisions to the recorded spectra was vanishingly small. This was ensured by fixing the upper-bound density of the mixture ρ at the sum of the partial values $\rho_{Ne} = \gamma(\gamma+1)^{-1}\rho$ and $\rho_{Ar} = (\gamma+1)^{-1}\rho$ for which triple collisions were shown to be absent in previous experiments with pure neon [12–14] and pure argon [15,16].

We chose to define some "total binary intensity" according to $I_{(2)} = S_{(2)}/\rho_{Ne}\rho_{Ar}$. It was generally extracted through a study of the noise-corrected "density-normalized" scattering signal against density. An illustration is given in Figure 2. The four curves show that at 15, 25, 35, and 45 cm^{-1} and for a mixture of concentration $\gamma = 4$, neither monomeric contributions (value of the curve at zero density) nor three-body contributions (negative curvature for high densities) were
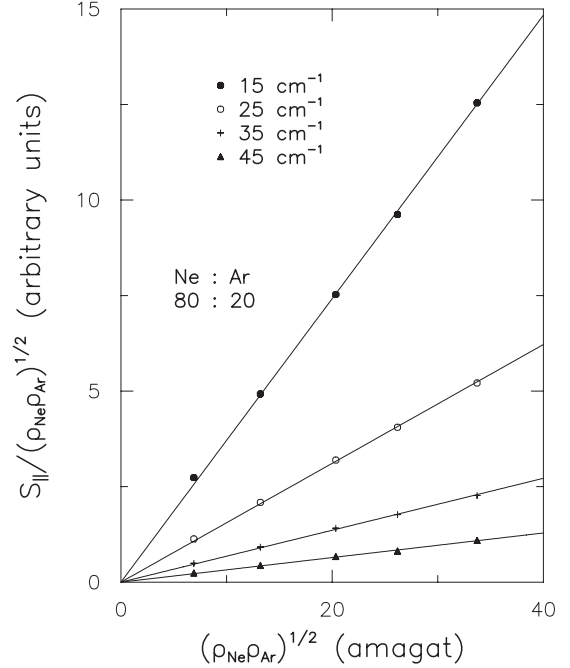

FIG. 2. Noise-corrected "density-normalized" overall anisotropic signal, $S_{\parallel}/\sqrt{\rho_{Ne}\rho_{Ar}}$ (arbitrary units), as a function of $\sqrt{\rho_{Ne}\rho_{Ar}}$ (amagat), for $\gamma = \rho_{Ne}/\rho_{Ar} = 4$. Four curves are shown, corresponding to the measurements taken at $\nu = 15$, 25, 35, and 45 cm^{-1}. The perfect linearity of these curves offers evidence that, in the displayed density and frequency ranges, the recorded signal $S_{\parallel}$ is nothing else but the binary signal, $S_{(2)}$, defined in the text.

present below $\rho = 35$ amagat. For each frequency shift, $I_{(2)}$ was reliably extracted from the slope of the linear curve, and was calibrated in absolute units (cm^6) using as a reference the integrated intensity of the $S_0(0)$ rotational line of H_2 [11,42].

By means of Eq. (7), one thus has:

$$I_{NeAr} = I_{(2)} - \frac{\gamma}{2}I_{NeNe} - \frac{1}{2\gamma}I_{ArAr}, \qquad (8)$$

where I_{NeAr}, I_{NeNe} and I_{ArAr} are now absolute-unit intensities, either anisotropic or isotropic. The intensities I_{NeNe} and I_{ArAr} were taken from studies on pure gaseous neon [12–14] and argon [15,16], respectively.

Neon was favored in the mixture in order to partially compensate the fact that intensities by Ar-Ar are much greater than those by Ne-Ne, which is a behavior susceptible to erroneous intensities by Ne-Ar. Specifically, three values of concentration ratio, $\gamma = 9$, 4, and 65/35 ($\pm 0.2\%$), were used over the respective ranges of frequency shift [5:15], [5:300] and [250:300] cm^{-1} in order to ensure that $\frac{\gamma}{2}I_{NeNe}$ and $\frac{1}{2\gamma}I_{ArAr}$ were of the same order of magnitude. The fact that all different values of γ led to sensibly identical intensities I_{NeAr} was evidence that our extraction procedure meets the most stringent validation criteria.

The gas density of the mixture, ρ (in amagat), was deduced from the measured pressure P using the second order virial expansion of the gas. According to the notations by Dymond and Smith [43], in the case of a mixture $a:b$, the
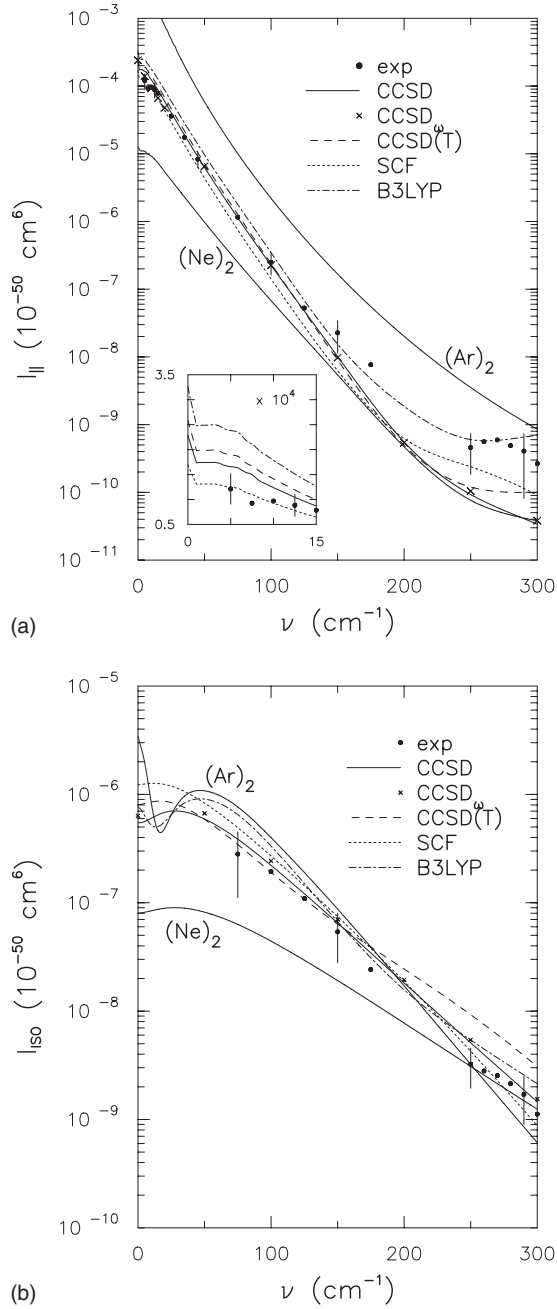
(a)

(b)

FIG. 3. Ne-Ar absolute-unit CIS intensities (cm^6) as a function of frequency shift (cm^{-1}). Vertical lines represent experimental uncertainties. (a) Anisotropic intensities. The 0–15 cm^{-1} spectral range is enhanced in order to highlight the contribution of the bound and predissociating dimers. A full width at half maximum of 1 cm^{-1} was taken for the slit function to mimic the aperture used. (b) Isotropic intensities.

second and third virial coefficients read, respectively:

$$B = B_{aa}x_a^2 + 2B_{ab}x_ax_b + B_{bb}x_b^2, \qquad (9)$$

$$C = C_{aaa}x_a^3 + 3C_{aab}x_a^2x_b + 3C_{abb}x_ax_b^2 + C_{bbb}x_b^3, \qquad (10)$$

where x_a and x_b are the molar fractions of the constituents a and b. The second and third virial coefficients for pure gas-

TABLE I. Experimental absolute-unit CIS intensities (cm^6), both anisotropic, $I_\parallel$, and isotropic, I_{iso}, and depolarization ratio, η, of Ne-Ar as a function of frequency shift, ν(cm^{-1}).

ν (cm^{-1})	$I_\parallel$ (cm^6)	I_{iso} (cm^6)	η
5	1.21×10^{-54}		0.981
7.5	9.26×10^{-55}		1.145
10	9.67×10^{-55}		1.058
12.5	8.83×10^{-55}		0.998
15	7.85×10^{-55}		0.907
25	3.60×10^{-55}		0.944
35	1.75×10^{-55}		0.918
45	8.31×10^{-56}		0.920
75	1.16×10^{-56}	2.81×10^{-57}	0.714
100	2.49×10^{-57}	1.94×10^{-57}	0.520
125	5.27×10^{-58}	1.10×10^{-57}	0.315
150	2.32×10^{-58}	5.39×10^{-58}	0.295
175	7.22×10^{-59}	2.42×10^{-58}	0.230
250	4.59×10^{-60}	3.24×10^{-59}	0.131
260	5.60×10^{-60}	2.80×10^{-59}	0.171
270	5.95×10^{-60}	2.54×10^{-59}	0.193
280	4.88×10^{-60}	2.13×10^{-59}	0.190
290	4.07×10^{-60}	1.70×10^{-59}	0.196
300	2.66×10^{-60}	1.12×10^{-59}	0.195

eous neon, $B_{NeNe} = 11.346$ cm^3 mol^{-1} and $C_{NeNeNe} = 221.1$ cm^6 mol^{-2} [44], and pure gaseous argon, $B_{ArAr} = -16.2705$ cm^3 mol^{-1} and $C_{ArArAr} = 989.25$ cm^6 mol^{-2} [45], as well as the second virial coefficient for the heteronuclear pairs, $B_{NeAr} = 10.479$ cm^3 mol^{-1} [46], were obtained by interpolating the most appropriate Pressure-Vapor-Transfer (PVT) data available at the working temperature. The third coefficients C_{NeNeAr} and C_{NeArAr} were taken as the geometric mean of their pure gas counterparts [47]:

$$C_{aab} = (C_{aaa}^2 C_{bbb})^{1/3}, \qquad (11)$$

$$C_{abb} = (C_{aaa} C_{bbb}^2)^{1/3}. \qquad (12)$$

IV. RESULTS

Figure 3 shows the Stokes side of the anisotropic [Fig. 3(a)] and isotropic [Fig. 3(b)] Ne-Ar spectrum, $I_{NeAr}(\nu)$. Experimental intensities are given in Table I over the ranges [5:300] cm^{-1} and [75:300] cm^{-1}. The lower bounds $\nu = 5$ and 75 cm^{-1} were imposed by the lowest values of frequency shift probed in the aforemeasured anisotropic and isotropic spectra of (Ar)$_2$ [15] and (Ne)$_2$ [14], respectively. Use of a photomultiplier (PM) was made to record the spectra over low and intermediate frequency shifts. A highly sensitive coupled-charged device (CCD) was required beyond 200 cm^{-1} to detect the weak light scattering signal in the wing of the spectrum [11,12]. Spectral resolution of the spectrometer was gradually increased from 1 cm^{-1} to 10 cm^{-1} as

TABLE II. Ne-Ar n^{th}-order spectral moments (Å^9 s^{-n}), anisotropic, $M_{n\parallel}$, and isotropic, $M_{n,iso}$.

	$M_{n\parallel}$				
n	0 (Å^9)	1 (10^{11} Å^9 s^{-1})	2 (10^{25} Å^9 s^{-2})	3 (10^{37} Å^9 s^{-3})	4 (10^{51} Å^9 s^{-4})
Experiment	$1.8 \pm 25\%$	$3.5 \pm 25\%$	$2.7 \pm 30\%$	$3.7 \pm 30\%$	$2.9 \pm 40\%$
CCSD[a]	2.16	3.71	2.87	3.13	2.46
CCSD(T)[b]	2.46	4.21	3.26	3.49	>2.74
SCF[b]	1.60	2.63	2.04	2.16	>1.70
B3LYP[b]	3.13	5.60	4.34	5.47	⩾4.38
	$M_{n,iso}$				
n	0 (10^{-3} Å^9)	1 (10^{10} Å^9 s^{-1})	2 (10^{23} Å^9 s^{-2})	3 (10^{36} Å^9 s^{-3})	4 (10^{50} Å^9 s^{-4})
Experiment	$3.3 \pm 60\%$	$0.79 \pm 50\%$	$6.3 \pm 45\%$	$5.1 \pm 45\%$	$5 \pm 50\%$
CCSD[a]	4.89	1.02	8.14	6.46	>5.37
CCSD(T)[b]	5.37	1.06	8.49	8.31	>7.03
SCF[b]	7.55	1.23	9.79	6.58	>5.40
B3LYP[b]	6.25	1.36	10.8	7.92	>6.65

[a]Spectral moments calculated by the authors with data taken from Ref. [25].
[b]Spectral moments calculated by the authors with data taken from Ref. [26].

frequency shift was increased from 5 cm^{-1} to 200 cm^{-1}. Upon using the CCD, the resolution of the spectrograph was fixed at 1.2 cm^{-1}.

The procedure of extracting Ne-Ar signals, albeit its difficulty, provided measurements that varied smoothly with ν, except for the wing of the weak isotropic spectrum. As expected, measurement dispersion for that spectrum is larger than was for the anisotropic spectrum.

A. Anisotropic intensities

Upon comparison between theory and experiment [Fig. 3(a)], piecewise agreement is found for each of the models over specific spectral regions. Over the range $[5:15]$ cm^{-1}, SCF seems best to reproduce observation, while over the range $[15:125]$ cm^{-1} this role is rather taken over by the two correlation-consistent coupled-cluster anisotropy models, CCSD and CCSD(T), whose related spectra were almost indistinguishable. Laser-frequency dependence does not seem to be significant. Finally, over the range $[150:300]$ cm^{-1}, it is the B3LYP function which produces the best results, whereas any other model turns out to underestimate observation. Interestingly, the B3LYP spectrum differs from the measured one by an almost constant factor of 0.5 over the whole covered frequency interval. This shows that the numerically cheap DFT can be of some interest at least as far as qualitative trends are considered [26].

Table II reports values of zeroth-order, first-order, second-order, third-order, and fourth-order spectral moments calculated from the theoretical spectra, and compares them with those extracted from our measurements through the expression:

$$M_{n\parallel} = \frac{15}{2}\left(\frac{\lambda_L}{2\pi}\right)^4 (2\pi c)^n \int_{-\infty}^{\infty} I_{\parallel}(\nu)\nu^n d\nu, \quad (13)$$

for $n=0$, 1, 2, 3, and 4, and for a laser wavelength $\lambda_L =514.5$ nm. Given the quantum treatment here offered, odd-order moments are not zero, and even more so for a nonclassical system such as the one treated here. The comparison confirms that low-frequency shifts, mainly contributing to $M_{0\parallel}$, are best described by the SCF method, whereas the higher ranges of frequency shift, mainly affecting high-order moments, are best represented by the CCSD and CCSD(T) response approaches. From the measured $M_{0\parallel}$, the value $B_K^{(0),\alpha^2}=2.48\times10^{-13}$ cm^9 erg^{-1} mol^{-2} was deduced [48], which is a meaningful approximation of the Kerr second virial coefficient of Ne-Ar at room temperature. This value is 20% below $B_K^{(0),\alpha^2}=3.07\times10^{-13}$ cm^9 erg^{-1} mol^{-2}, which is the value predicted by theory after interpolation of the data of Ref. [27] at $T=294.5$ K. According to the data reported in [27], $B_K^{(0),\alpha^2}$ is by far the dominant contribution to the Kerr second virial coefficient of Ne-Ar, containing more than 85% of its total value, either static one ($B_K^{(0)}=2.76 \times10^{-13}$ cm^9 erg^{-1} mol^{-2}) or dynamic one ($B_K^{(\omega)}=2.68 \times10^{-13}$ cm^9 erg^{-1} mol^{-2}), at the working conditions of temperature and incident beam wavelength. The aforegiven value of $B_K^{(0),\alpha^2}$ is sensibly the same as the one obtained by integrating the spectrum of the CCSD anisotropy representation of Ref. [25].

CCSD spectra were also computed for $(Ne)_2$ and $(Ar)_2$, and are now compared to the one for Ne-Ar. For small values of ν, Ne-Ar exhibits intensities of one whole order of magnitude higher and lower than the respective intensities of

$(Ne)_2$ and $(Ar)_2$. At larger values of ν, its intensities get closer to the ones of $(Ne)_2$. The experimental Ne-Ar anisotropic spectrum features a clearly changing slope just below the frequency shift $\nu = 250$ cm^{-1}. This behavior by no means is an artifact of extraction signals in the procedure analysis. In fact, a similar characteristic feature is also predicted theoretically by the best anisotropy representations for Ne-Ar and $(Ne)_2$, and was also observed experimentally in the latter system [13]. The slope break observed in the spectral wing of this pair should lie with the pattern of the "bump" which characterizes the corresponding anisotropy functions at close separations.

B. Isotropic intensities and depolarization ratio

Figure 3(b) allows one to compare theory to experiment in the case of the isotropic spectrum. As a general remark, quantum-mechanical predictions are satisfactory. Over the range $[75 : 150]$ cm^{-1}, experiment is fairly well reproduced by CCSD(T) and CCSD, whereas beyond 250 cm^{-1} good agreement is obtained only with the CCSD model. Once again, the economical DFT method to some extent reproduces the experiment, resulting in intensities that differ from the measurements by a constant factor of 0.75 over the whole interval of ν.

The experimental isotropic moments $M_{0,iso}$, $M_{1,iso}$, $M_{2,iso}$, $M_{3,iso}$, and $M_{4,iso}$, given in Table II, are estimates. This is because convergence was not fully ensured at 300 cm^{-1} for $M_{3,iso}$ or $M_{4,iso}$, and also no measurements below 75 cm^{-1} were accessible. Nevertheless, the comparison between these values and the ones obtained from the models seems to corroborate the relevance of the CCSD trace model.

Figure 4 illustrates the Ne-Ar depolarization ratio, η, as a function of ν. The depolarization ratio deduced from the measurements is steadily above any prediction, as expected from the characteristics of the corresponding isotropic spectra. Its values are given in the last column of Table I. Theoretical predictions, on the basis of the sophisticated coupled-cluster method, turn out to reproduce fairly well experiment over the range $[75 : 125]$ cm^{-1}. This is no more the case in the far wing, where experiment displays a minimum six times more intense than the minimum predicted by CCSD and CCSD(T). Such a minimum, observed in the wing of Ne-Ar, was already observed in $(Ne)_2$.

V. CONCLUSION

This paper is intended to better the understanding of the role of monoatomic gas mixtures in planetary atmospheric environments. We reported the long-overdue collision-induced Raman scattering spectrum, along with the depolarization ratio of the Ne-Ar pair at room temperature. To this end, we carried out an exhaustive joint experimental/
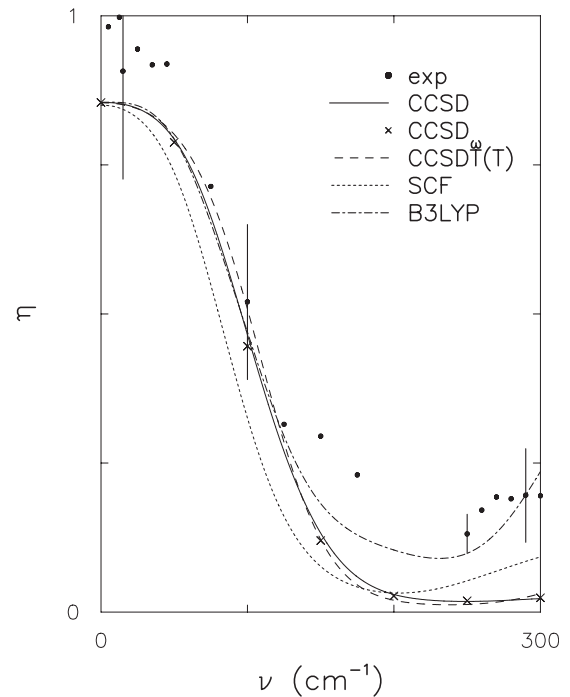

FIG. 4. Depolarization ratio of Ne-Ar as a function of frequency shift (cm^{-1}). Vertical lines represent experimental uncertainties. Shown experimental errors, in ascending ν order, are $\pm 20\%$, $\pm 25\%$, $\pm 25\%$, and $\pm 40\%$.

theoretical study of the Ne : Ar gas mixture, for three different concentration ratios and for overall densities varying from 15 to 140 amagat, in order to guarantee a reliable extraction of the Ne-Ar spectrum over a broad interval of frequency shift. Both the anisotropic and the particularly weak isotropic intensities were recorded, and then were used to check the relevance of available anisotropy and trace polarizability computations. The similar trends we noticed between the anisotropy models for Ne-Ar and $(Ne)_2$ on one hand, and between the trace models for Ne-Ar and $(Ar)_2$ on the other hand were naturally transposed to the spectra. Despite the satisfactory predictions of CCSD and CCSD(T) over a large range of frequency shift, large discrepancies were observed in the wing. This suggests that even the best-to-date pair-polarizability functions of Ne-Ar still lack some significant amount of dynamical electronic correlation at separations close to the unified atom limit. The opposite trend was observed with density functional theory, found to reproduce fairly well the experiment in the spectrum wing but to systematically overestimate it elsewhere. From our measurements, an approximate value for the Kerr second virial coefficient of Ne-Ar was deduced, which to the best of our knowledge is the first experimental observation for that property.

[1] Z. J. Kiss and H. L. Welsh, Phys. Rev. Lett. **2**, 166 (1959).

[2] D. R. Bosomworth and H. P. Gush, Can. J. Phys. **43**, 729 (1965).

[3] L. Frommhold, *Collision-induced Absorption in Gases* (Cambridge University Press, Cambridge, 1993).

[4] J. P. C. McTague and G. Birnbaum, Phys. Rev. Lett. **21**, 661 (1968).

[5] J. P. C. McTague and G. Birnbaum, Phys. Rev. A **3**, 1376 (1971).

[6] M. H. Proffitt and L. Frommhold, Phys. Rev. Lett. **42**, 1473 (1979).

[7] M. H. Proffitt and L. Frommhold, J. Chem. Phys. **72**, 1377 (1980).

[8] L. Frommhold and M. H. Proffitt, Phys. Rev. A **21**, 1249 (1980).

[9] F. Rachet, M. Chrysos, C. Guillot-Noël, and Y. Le Duff, Phys. Rev. Lett. **84**, 2120 (2000).

[10] C. Guillot-Noël, M. Chrysos, Y. Le Duff, and F. Rachet, J. Phys. B **33**, 569 (2000).

[11] F. Rachet, Y. Le Duff, C. Guillot-Noël, and M. Chrysos, Phys. Rev. A **61**, 062501 (2000).

[12] F. Rachet, M. Chrysos, G. Lothon, R. Moszynski, and A. Milet, J. Raman Spectrosc. **34**, 972 (2003).

[13] S. Dixneuf, F. Rachet, and M. Chrysos (unpublished).

[14] F. Rachet, S. Dixneuf, and M. Chrysos (unpublished).

[15] F. Chapeau-Blondeau, V. Teboul, J. Berrué, and Y. Le Duff, Phys. Lett. A **173**, 153 (1993).

[16] O. Gaye, M. Chrysos, V. Teboul, and Y. Le Duff, Phys. Rev. A **55**, 3484 (1997).

[17] M. Chrysos, O. Gaye, and Y. Le Duff, J. Phys. B **29**, 583 (1996).

[18] M. Chrysos, O. Gaye, and Y. Le Duff, J. Chem. Phys. **105**, 31 (1996).

[19] T. Müller, *Computational Nanoscience: Do It Yourself!*, edited by J. Grotendorst, S. Blügel, and D. Marx, NIC series (John von Neumann Institute for Computing, Julich, 2006), vol. 31, p. 19.

[20] T. H. Dunning, Jr., J. Chem. Phys. **90**, 1007 (1989).

[21] T. H. Dunning, Jr., K. A. Peterson, and A. K. Wilson, J. Chem. Phys. **114**, 9244 (2001).

[22] C. Hättig, H. Larsen, J. Olsen, P. Jørgensen, H. Koch, B. Fernández, and A. Rizzo, J. Chem. Phys. **111**, 10099 (1999).

[23] C. Hättig, J. L. Cacheiro, B. Fernández, and A. Rizzo, Mol. Phys. **101**, 1983 (2003).

[24] B. Fernández, C. Hättig, H. Koch, and A. Rizzo, J. Chem. Phys. **110**, 2872 (1999).

[25] J. L. Cacheiro, B. Fernández, D. Marchesan, S. Coriani, C. Hättig, and A. Rizzo, Mol. Phys. **102**, 101 (2004).

[26] G. Maroulis and A. Haskopoulos, Chem. Phys. Lett. **358**, 64 (2002).

[27] A. Rizzo, S. Coriani, D. Marchesan, J. L. Cacheiro, B. Fernández, and C. Hättig, Mol. Phys. **104**, 305 (2006).

[28] By using the notations of Ref. [27].

[29] G. Herzberg, *Molecular Spectra and Molecular Structure, Part I: Spectra of Diatomic Molecules*, 2nd ed. (D Van Nostrand, Princeton, 1950).

[30] K. Fox and I. Ozier, J. Chem. Phys. **52**, 5044 (1970).

[31] S.-I. Tomonaga, *The Story of Spin* (University of Chicago Press, Chicago, 1998).

[32] A. Barrow and R. A. Aziz, J. Chem. Phys. **89**, 6189 (1988).

[33] R. A. Aziz and M. J. Slaman, Chem. Phys. **130**, 187 (1989).

[34] R. A. Aziz and M. J. Slaman, J. Chem. Phys. **92**, 1030 (1990).

[35] G. Maroulis, J. Phys. Chem. A **104**, 4772 (2000).

[36] L. Frommhold, Adv. Chem. Phys. **46**, 1 (1981).

[37] These values were estimated by plotting, as a function of r, the quantities $F^n(\beta)$ and $G^n(\alpha)$, which are implied in the calculation of the nth-order anisotropic and isotropic moments [38,39]. We thus observed that F^n and G^n, $n = 0, 2, 4, 6$, get a zero value below 4, 4.5, and 5 bohr for $(Ne)_2$, Ne-Ar, and $(Ar)_2$, respectively. As moments are not seen to be affected by separations below those bounds, spectra are not expected to be affected either.

[38] U. Bafile, R. Magli, F. Barocchi, M. Zoppi, and L. Frommhold, Mol. Phys. **49**, 1149 (1983).

[39] C. G. Joslin, J. D. Goddard, and S. Goldman, Mol. Phys. **89**, 791 (1996).

[40] In practice, this combination was slightly corrected in order to account for the aperture of the scattering angle [41].

[41] M. H. Proffitt, J. W. Keto, and L. Frommhold, Can. J. Phys. **59**, 1459 (1981).

[42] Since signals by pairs of unlike atoms scale with density as $\rho_a \rho_b$ whereas signals by pairs of like atoms scale as $\rho_a^2/2!$, the factor 14/45 in Eq. (4) of Ref. [11] should be halved.

[43] J. H. Dymond and E. B. Smith, *The Virial Coefficients of Pure Gases and Mixtures: A Critical Compilation, Published by Oxford University Press* (Watton Street, Oxford, 1980).

[44] A. Michels, T. Wassenaar, and P. Louwerse, Physica Grav. **26**, 539 (1960).

[45] A. Michels, H. Wijker, and H. K. Wijker, Physica Grav. **15**, 627 (1949).

[46] H. Schmiedel, R. Gehrmann, and B. Schramm, Ber. Bunsenges. Phys. Chem **84**, 721 (1980).

[47] J. Brewer and G. W. Vaughn, J. Chem. Phys. **50**, 2960 (1969).

[48] To that purpose, use was made of the formula $B_K^{(0),\alpha^2} = 2\pi\mathcal{N}^2 M_{0\parallel}/(405 k_B T)$ (CGS), which describes the major contribution to the static Kerr second virial coefficient component [27]; $\mathcal{N}$ is Avogadro's number.